*Chinese Journal of Chemistry*, **2004**, *22*, 913—919

**Article**

# Undistorted Cyclic Voltammograms at Scan Rates up to 2.5 MV•s$^{-1}$ through Positive Feedback Compensation of Ohmic Drop†

GUO, Zhi-Yong(郭智勇) LIN, Xiang-Qin*(林祥钦) DENG, Zhao-Xiang(邓兆祥)

*Department of Chemistry, University of Science and Technology of China, Hefei, Anhui 230026, China*

A circuit based on the current feedback operational amplifier was constructed to accomplish on-line ohmic drop compensation in ultrafast cyclic voltammetry. Firstly, its characteristics were confirmed experimentally on dummy cells. Then the reduction of anthracene in acetonitrile, a classical test example with very fast electron-transfer kinetics, was examined to prove them too. The results showed that this circuit could afford excellent ohmic drop compensation so that the undistorted voltammograms up to 2.2 MV•s$^{-1}$ scan rate can be recorded, and 2.5 MV•s$^{-1}$ if 5% error is tolerated.

**Keywords** ultrafast cyclic voltammetry, megavolt per second scan rate, ultramicroelectrode, instrument, ohmic drop compensation

## Introduction

Though being the simplest voltammetric technique, cyclic voltammetry provides lots of electrochemical information especially in the study of the thermodynamic and kinetic processes and the detection of electrogenerated transient intermediates.[1] Clearly, the more rapid the scan rate is employed, the faster the reactions can be studied. Indeed, a timescale $RT/Fv$ ~25 ns of the Faradaic response will be reached corresponding to a scan rate $v$ of 1 MV•s$^{-1}$, which means that the method may be performed up the nanosecond time domain to deepen the cognition of heterogeneous and homogeneous reactions. Furthermore, the thickness of the diffusion layer corresponding to the scan rate of megavolt per second for an average diffusion coefficient of *ca.* $10^{-5}$ cm$^2$•s$^{-1}$ is in the range of a few nanometers comparable to that of the double layer. While restricting the application of high scan rates, the possible coupling and interaction of the two layers also provide the possibility for further development of electrochemical theories and techniques.[2-4] However, it had being seen valueless because of serious voltammetric distortion in early experimental results, until the advent of ultramicroelectrodes in 1980s and the ensuing application of several related techniques such as instrument construction,[2,5-7] digital simulation,[8,9] background subtraction,[10] bandpass correction[11] and ohmic drop compensation[2,6,12-14] in recent twenty years.

Distortion of ultrafast cyclic voltammetry mainly stems from the solution ohmic drop $IR_s$, the time constant $R_sC_d$ of the electrochemical cell, interference of the capacitive and Faradaic currents and low-pass filter of the circuit. Among those, the latest could be eliminated mostly by using the good instruments and designing the suitable circuit, while the others all rest with the solution resistance $R_s$. At a disk ultramicroelectrode, the current $I$ and the capacitance of double layer $C_d$ are proportional to the electrode area, *i.e.* $r^2$, while $R_s$ is reciprocal to the electrode radius $r$, thus, $IR_s \propto R_sC_d \propto r \to 0$ when $r \to 0$.[15] However, $r$ can not be decreased at will to make $IR_s$ and $R_sC_d$ as small as possible because steady state spherical diffusion comes into the existence only if $r^2 >> DRT/Fv$.[2] In the usual experimental conditions of ultrafast cyclic voltammetry at scan rates up to megavolt per second, $R_s$ is about a few kilohms and $I$ is about a few to a few tens microamperes. Thus $IR_s$ can be about one hundred millivolts or more. Therefore, the ohmic drop and the cell time constant are still vital obstacles when the scan rate reaches the level of megavolt per second unless $R_s$ could be compensated in the majority (at least 90%—95%).[4,16,17]

Though valuable information could be extracted by the digital simulation and deconvolution, directly obtaining undistorted voltammograms by cancelling out ohmic drop is still an important object in this research domain, which has been carried out through on-line electronic positive feedback and current interruption technique as well as iterative correction of the applied potential. As the scan rate of the current interruption method is confined to a few kilohertz and an arbitrary waveform generator is needed for the iterative correc-

* E-mail: xqlin@ustc.edu.cn
Project supported by the National Natural Science Foundation of China (No. 20173054).
Received October 23, 2003; revised March 23, 2004; accepted May 20, 2004.
† Dedicated to Professor Chengye Yuan on the occasion of his 80th birthday.

tion of the applied potential, the electronic positive feedback method is the most widely used for its simplicity. Several potentiostat designs[2,6,12,14] through this method have gradually reached the scan rate range of megavolt per second with full ohmic drop compensation and negligible bandpass distortion.

In this work, a circuit based on current feedback operational amplifier with the positive feedback compensation of the ohmic drop was established to obtain undistorted voltammograms at as high scan rate as possible. Since we just wanted to examine the properties and limitation of this circuit that provides the possibility of exploring electrochemistry in ns time scale and nm space scale, special experimental conditions were chosen as suggested by Amatore *et al.*[2] to avoid the coupling of the diffusion layer and the double layer.

## Experimental

### Chemicals

Acetonitrile (HPLC quality) was distilled from calcium hydride and then degassed by nitrogen just before use. Tetraethylammonium tetrafluoroborate was commercially available (Aldrich), and it was dried at 60 ℃ under vacuum and stored in vacuo desiccator. Anthracene was purchased from Sigma Co. and recrystallized before use.

### Cell and apparatus

A two-electrode cell was made of a glass tube as described previously.[2] It was directly mounted on the printed circuit board (PCB) to shorten electrical leads and lessen connectors, which would keep the stray capacitance small and the propagation time short. The auxiliary electrode (Pt wire, 1 mm diameter) was installed on the back of PCB, the opposite side of signal and power layer, to decrease possible stray capacitance. A gold disk ultramicroelectrode acting as the working electrode was made of a 2.5 μm radius gold wire (Goodfellow Metals) according to the published method.[8] The working electrode was polished with 0.05 μm of alumina slurry on a cloth pad, ultrasonicated and rinsed with distilled deionized water and pure solvent prior to collecting voltammgrams.

A septum made of polytetrafluoro ethylene with the proper dimension and two holes, one for a Teflon tube and the other for the working electrode, was placed on the top of the cell in experimental processes. Nitrogen saturated by acetonitrile was sent through the Teflon tube to degas the solution and maintain the atmosphere during the experiments.

Potential waveforms were generated by a Model G305 waveform generator (10 MHz, HUNG CHANG, Korea) and a Model GRG-450B RF signal generator (GOODWILL, Taiwan) when the frequency was higher than 10 MHz. Voltammetric data were acquired on a Tektronix Model TDS220 digitizing oscilloscope with 100 MHz bandpass. Data were downloaded and stored by a personal computer for further analysis. Not bringing any distortion, all the voltammograms shown here were averaged 128 times to increase the signal-to-noise ratio.

The circuit described as follows was designed elaborately on a PCB. Surface-mounted electronic components instead of through-hole ones and SMA connectors were used for better high-frequency performance. The circuit was placed in a Faraday cage during the experiments, though no perceptible distortion was found without it.

### Physical description of the circuit

Because $R_s=\rho_s/4r$ suggests that the solution resistance is concentrated on the very surface of electrodes, it is nearly impossible to compensate the solution resistance of ultramicroelectrodes by a three-electrode cell. Thus a two-electrode cell system was employed to improve the bandwidth and stability of the overall system. Of course, this circuit could be reconstructed to a three-electrode cell system easily if only a reference electrode was directly linked to the inverting input pin of the potentiostat. An input buffer (not shown in Figure 1) was used to avoid re-injection of potential by the potentiostat and smooth the potential signal at each slope discontinuity. Noting that the potential-time variations should be recorded after the buffer to eliminate the time lag due to the buffer.

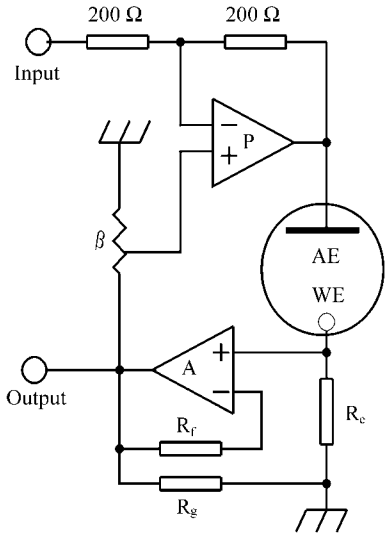


**Figure 1** Scheme of the circuit employed. P: the potentiostat (MAX4100). A: current measurer (MAX4224). WE, AE: working and auxiliary electrodes.

The complete system, as shown in Figure 1, just consisted of a potentioatat, an electrochemical cell and a current measurer. The operational amplifiers (opamp) were used according to technical notes of the manufacturer. The potentiostat was established with a voltage feedback opamp MAX4100. Its input impedance is much larger than that of a current feedback which makes it proper to act as a summing amplifier. The current measurer was done with a current feedback opamp. In contrast with usual value 10 kΩ of feedback resis-

tance if a voltage feedback opamp is used to achieve signals of the same intention, 130 Ω feedback resistance of MAX4224 is much lower, which makes the bandwidth greatly increased. Moreover, the stability is thus increased for its insensitivity to stray capacitances. Values of feedback resistor $R_f$ (130 Ω) and gain resistor $R_g$ (15 Ω) and sampling resistor $R_e$ (1 kΩ) were chosen as follows: Gain $G=1+R_f/R_g$ should not be too large to achieve good bandwidth. Thus $R_e$ should not be too small to make the output voltage large enough to compensate $R_s$. However, $R_e$ should not be too large so as to be negligible vis-à-vis the input impedance of the amplifier A (*ca.* 750 kΩ). Thus above values were decided through a series of optimizing to balance the needs of all sides.

In this circuit, compensative voltage $V_{com}$ proportional to the current $i$ is fed back to the non-inverting pin of the potentiostat to sum to the voltage $V_d$ delivered by the function generator. Thus the output voltage of the potentiostat $V_a=V_d+V_{com}=V_d+R_c i=V_d+2\beta(1+R_f/R_g)\times R_e i$, in which $R_c$ is the "compensation" resistance and $\beta$ the feedback ratio. As $R_c$ is increased upon raising $\beta$, oscillations appear. Just then $R_c=R_s+R_e+R_o$, while the "overcompensation" resistance $R_o=1/\omega C_d$, where $C_d$ is the double layer capacitance which could be calculated out according to the charging current $i_c=vC_d$ and $\omega$ is the band-pass pulsation which could be worked out by studying dummy cells with known resistance. Hence, perfect compensation will be achieved if we increase $R_c$ by adjusting $\beta$ continuously until sustained oscillations appear and subsequently decrease it by an amount equal to $R_o$.[6]

## Results and discussion

### Bandpass and time lag of the circuit

The set of data was recorded with 1 V amplitude sinusoidal tension. The values of components of the dummy cell were selected so that values of the capacitance and the resistance corresponded to those observed experimentally at the electrode investigated in this study. The upper horizontal scale in Figure 2 indicated the values of triangle-wave scan rate, $v$, corresponding to the sine-wave frequency, $f$, shown on the lower horizontal scales through the relationship $f$ (Hz)$\approx 4v/(\mathrm{V\cdot s^{-1}})$, given for a single electron transfer.[10] The Bode plots showed that this circuit behaved approximately as a second-order filter (*i.e.* with about negative slopes of 40 dB per decade for frequencies higher than the cutting frequency $f_0$). Because $f_0$ is about 28 MHz, the highest usable scan rate is about 7 $\mathrm{MV\cdot s^{-1}}$. The similar frequency-response relation of a pure $R$ dummy cell and an $RC$ one indicated that this circuit has strong ability to drive capacitive loads.

Time lag $t_{lag}$ is a very important factor in ultrafast cyclic voltammetry because it will change the positions of positive and negative peaks, which are just used to determine thermodynamic and kinetic parameters. Fortunately, $t_{lag}$ does not alter voltammetric shapes. Thus it could be easily corrected by translating the potential axis $+vt_{lag}$ in the negative scans and $-vt_{lag}$ in the positive scans. $t_{lag}$ includes two additive components as described,[2] one is the time lag due to the phase shift angle caused by circuit distortion and the other "mechanical" delay. In the practice, it is unnecessary to tell them apart, so they are counted together in this paper. The $t_{lag}$ was determined as follows: cyclic triangular potential input of different frequency was used to pass a pure $R$ dummy cell, thus the output signal was triangular wave too. Then the distance between slope discontinuities of the input and output signals was just $t_{lag}$. The data are shown in Figure 3 and used for correction.

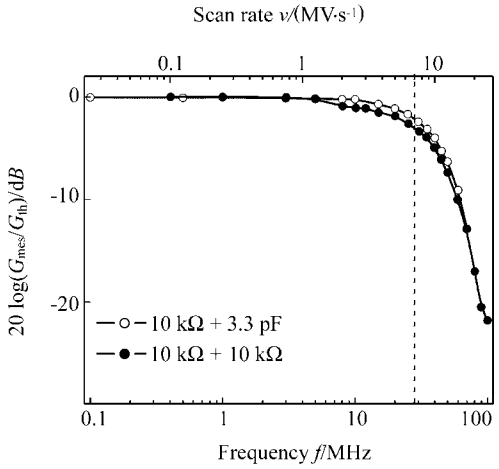


**Figure 2** Bode plots for the circuit connected to dummy cells. The vertical line represents the cutting frequency ($f_{-3dB}$=28 MHz) corresponding to the usable scan rate $v$=7 $\mathrm{MV\cdot s^{-1}}$.

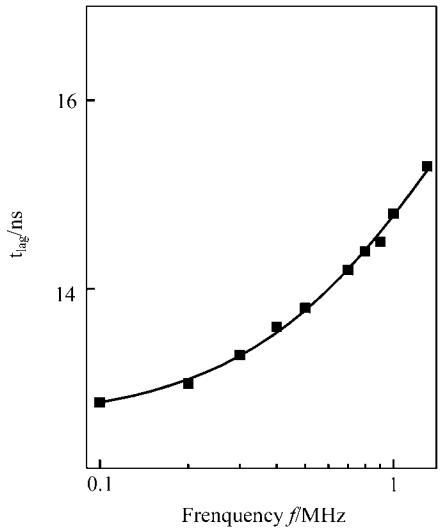


**Figure 3** Total time lag $t_{lag}$ of this circuit as a function of the frequency of the triangular wave used.

### Compensation effect

As the compensation effect was the most important subject, three methods described as follows were used to examine it.

Performing cyclic voltammetry under conditions where no Faradaic current is observed is the easiest way. In such cases, an ideal electrochemical system should behave as a pure *RC* series circuit, *R* being the uncompensated resistance and *C* being the double layer capacitance. If 100% compensation is achieved, *i.e.* $R=0$, the response will resemble a perfect square pulse and the charging current *i* is equal to *vC*. It is well shown in Figure 4. All the experimental data were a little larger than the theoretical data. It was caused by the stray capacitance. From the difference between them, the amount of the stray capacitance could be roughly estimated as about 0.2—0.3 pF.

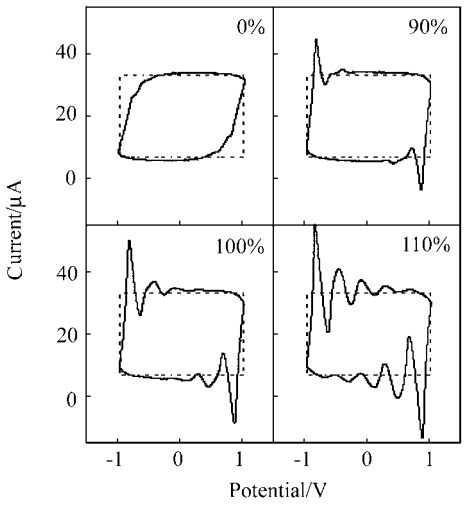


**Figure 4** Experimental (solid lines) and theoretical (dashed lines) current variations with potential applied shown for various levels (indicated on each panel) of compensation at 4 $MV \cdot s^{-1}$ when the circuit is connected to a pure *RC* dummy cell ($R=10$ kΩ, $C=3.3$ pF).

Various frequency sinusoidal waves in the range of 10 MHz acting as input signals, pseudo-impedance formed with different values of pure resistance or resistance in series with capacitance were determined when the compensation level was about 100%. Comparison between the theoretical and measured values is shown in Figure 5. Results showed the good consistency between them and thus proved the reliability of this circuit.

To examine compensation effect further, another method was applied. The dummy cell was constructed as follows: a pseudo-Faradaic impedance built by a resistance $R_F$ (10 kΩ) in series with a diode 1N4148, was parallel with $C_d$ (2 pF) and then in series with a resistance $R_s$ (10 kΩ). The above values were similar to experimental parameters. Thus the dummy cell could provide a rough simulation of a Faradaic reaction. The results were shown in Figure 6. It showed that Faradaic signal which was distorted by the ohmic drop such as that with 0% compensation could be effectively restored by this circuit. Comparing Figure 6 with Figure 4, we found that oscillation is somewhat damped after the pseudo-Faradaic impedance is introduced, suggesting that Faradaic impedance could enhance the stability of the circuit to a certain extent.

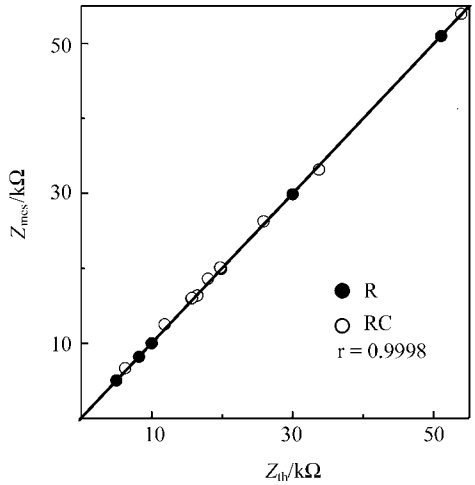


**Figure 5** Comparison between the theoretical values ($Z_{th}$) and the measured ($Z_{mes}$) of the pseudo-Faradaic impedance formed by a pure resistance or a resistance series with a capacitance.

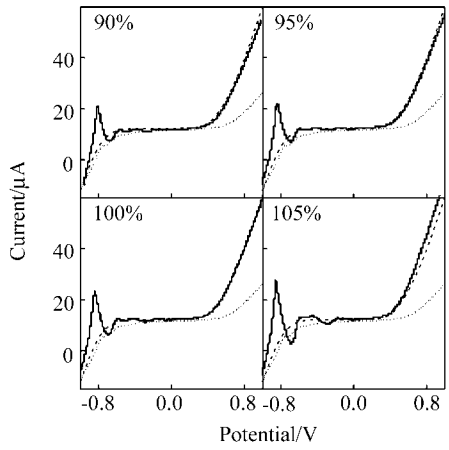


**Figure 6** The current-potential curves of a virtual dummy cell incorporating a pseudo-Faradaic component ($R_u=10$ kΩ, $C_d=2$ pF, $R_F=10$ kΩ) shown for various levels of compensation as indicated on each panel. Dotted lines: the uncompensated (0% compensation); solid lines: the compensated at various levels; dashed lines: the theoretical (theoretical 100% compensation, achieved by simulating the above dummy cell when $R_u=0$ by Protel).

### Determination of $R_s$

Although the compensating level could be judged by the oscillation, it is still helpful to the confirmation of compensation validity if $R_s$ could be determined precisely. $R_s$ and $C_d$ were obtained from the voltammetry of the solution in the absence of anthracene by measuring the cell time constant $\tau=R_sC_d$. Though this classic method is not able to reach the required precision because of the significant contribution of the circuit own time constant and band-pass in this range of time constants, it was not used just for determining compensating level but only proving compensation validity thus need not be too precise. The result is $R_s=(9.6\pm0.6)$ kΩ and $C_d=(3.4\pm0.2)$ pF for the solutions applied (ace-

tonitrile, [$NEt_4BF_4$]=0.9 mol/L) and the gold ultramicrodisk electrode with a nominal radius 2.5 μm. It accords with results of Amatore *et al.* very well,[2] and is consistent with the value 0.5—0.6 of $\beta$ determined experimentally too.

However, a puzzling problem appears. $\rho_s$ of the solutions applied (acetonitrile, [$NEt_4BF_4$]=0.9 mol/L) is approximately 20 Ω•cm,[18] thus the theoretical solution resistance would be about 20 kΩ according to $R_s=\rho_s/4r$. It is twice larger than the value determined experimentally. Then where on earth the great difference between them comes from? It stems from our simplifying the solution system to a pure *RC* dummy cell, that is, we usually consider that the cell obeys a classical Warburg diagram, *i.e.* a pure *RC*-series element circuit with the Faradaic impedance being placed in parrallel of the capacitor. This is what we also considered in deriving the potentiostat predicted responses for the real cell and what we mimicked with the dummy *RC* cell. In fact, a real cell equivalent electronic diagram is seldom a pure *RC*-series circuit but one generally much more complicated. Thus using such *RC* circuit consists only of suitable operative model of the "black-box" circuit of the real cell. Therefore, it is not surprising that the determined value of $R_s$ obtained experimentally within the framework of a pure *RC* model differs from that computed through using the reported solution resistivity and electrode size and geometry. Actually, the difference between the determined value and the theoretical one simply represents the degree of accuracy of the *RC*-equivalent model circuit towards the true "cell + electrode seals + connections + stray capacitances + *etc.*" circuit. In this case, the theoretical value is the true solution resistance, while the experimentally determined value would be its "effective" value within the *RC* equivalence. However, the theoretical value used within the simple framework of an *RC*-series circuit would not lead to correct operative values since then the real cell circuit should be used. Thus, for our purpose, since the *RC* equivalent circuit produces reasonably adequate fits to the transient experimental background current, and is coherent with the modeling of our circuit and its further use, it is technically correct and coherent. Therefore our procedure fulfills our needs for compensating the "effective" resistance and effective capacitance that is what matters electronically speaking within our *RC*-model of our cell. In a word, the value we measured is not the real solution resistance $R_s$, but conversely the effective value of the resistance of the equivalent *RC* circuit, which is the only one that does matter in our work.

**Megavolt voltammetry of anthracene-experimental demonstration of the validity of the circuit**

In recent years, being the fastest heterogeneous electron transfer reaction and a well-established electrochemical system, the reduction of anthracene in acetonitrile at gold electrodes has become a very popular one to test the performance of an ultrafast voltammetric circuit. Thus it was applied to check our circuit too. As the purpose of us was just to test the validity of the circuit and find out the maximum attainable scan rate, data stayed on the level of raw ones without applications of any other processing except that the effect of the time lag was corrected.

A series of 100% compensated voltammograms for the reduction of anthracene (18.0 mmol/L) in acetonitrile (0.9 mol/L $NEt_4BF_4$) at a gold ultramicroelectrode (nominal 5 μm diameter) covering the range of scan rates from 0.1 to 2.5 MV•$s^{-1}$ are shown in Figure 7. And a set of simulated voltammograms based on a self-established simulating program of our group[9,19,20] are also shown and compared with them. In these simulations, Butler-Volmer kinetics was observed with following parameters used: $E^0=-1.61$ V versus the Pt

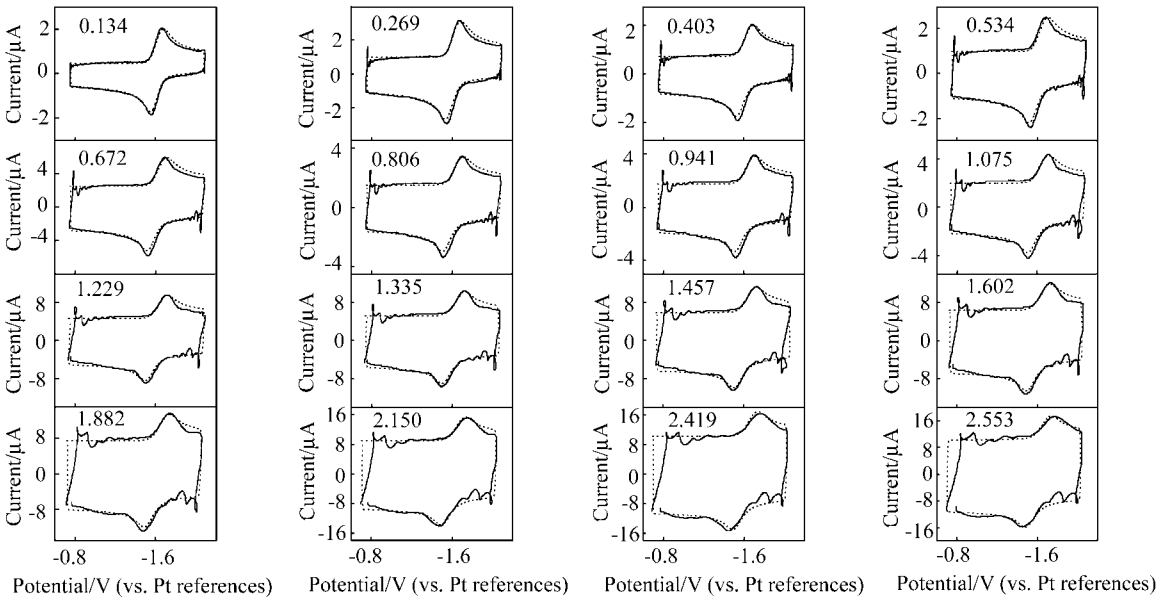


**Figure 7** Cyclic voltammograms of anthracene at different scan rates (as indicated on each panel in MV•$s^{-1}$). Solid curves: experimental at 100% compensation; dashed lines: simulated.

reference, $\alpha=0.45$, $k^0=5.1$ cm•s$^{-1}$, $D_O=D_R=1.6\times10^{-5}$ cm$^2$•s$^{-1}$, $r=2.6\pm0.1$ μm (determined by cyclic voltammograms at routine scan rates and data not shown here), $R_u$ = 0 (*i.e.* 100% compensation, without any ohmic drop), $C_d$ was an adjustable value in the range of 3.2—3.8 pF to fit the capacitive current trace to carry on the comparison between experimental voltammograms and simulated ones simply.

From this comparison, it was found that no obvious distortion was introduced even at scan rates up to 2.2 MV•s$^{-1}$. If 5% error is tolerated, then the scan rate will reach up to 2.5 MV•s$^{-1}$. In the panel for scan rates higher than 2 MV•s$^{-1}$, nonlinearity of triangular wave appreciably interferes with the Faradaic signals of the positive peak besides the damped oscillation. However, if an analog low-pass filter whose time constant was 62 ns was applied, the positive peak was still observable up to about 4 MV•s$^{-1}$ (the maximum scan rate available of our instruments). Because the variations of the peak-to-peak separation $\Delta E_p$ above 2.5 MV•s$^{-1}$ did not agree with the simulated ones to our satisfaction, those data are not shown while all data shown here are achieved without any filter.

Some portions of experimental voltammograms are not absolutely accordant with simulated ones. It is mainly attributed to non-linearity of the triangular wave. And this point could be proved if we observed carefully voltammograms shown in Figure 4. In fact, this kind of deviation is unimportant because the thermodynamic and kinetic information we are interested in is all included in voltammograms without any distortion.

Excellent performance of this circuit is also indicated in Figures 8 and 9, which show the $\Delta E_p$ and $E_p$ as a function of the scan rate. It can be seen that there is an excellent fit between the experimental data and the theoretical $\Delta E_p$ and $E_p$ *vs.* $\log[k^0/(FvD/RT)^{1/2}]$ curves[21] corresponding to $k^0=5.1$ cm•s$^{-1}$ up to a scan rate of 2.2 MV•s$^{-1}$. Above 2.2 MV•s$^{-1}$, the experimental points deviate more and more from the theoretical curves. However as described[22], it is difficult to make clear the source of the observed deviations because filtering effects due to the circuit and the progressive breakdown of the validity of Frumkin's approximation on steady diffusion-migration within the double layer appear together in the present conditions.

## Conclusion

In this work, a circuit was constructed to achieve on-line ohmic drop compensation for ultrafast cyclic voltammetry. Tests showed that a theoretical scan rate 7 MV•s$^{-1}$ and the highest experimental one 2.5 MV•s$^{-1}$ could be reached. Its utilization will allow direct meas urement of the fastest rates of electron transfer occurring in the nanosecond time domain from peak separations without resorting to deconvolution. Furthermore, it provides more possibility to carry out the research in the nanometer spatial domain, too. Clearly, being a real-time and *in situ* method, it will be helpful to chemical and biological studies involved in fast electron transfer.

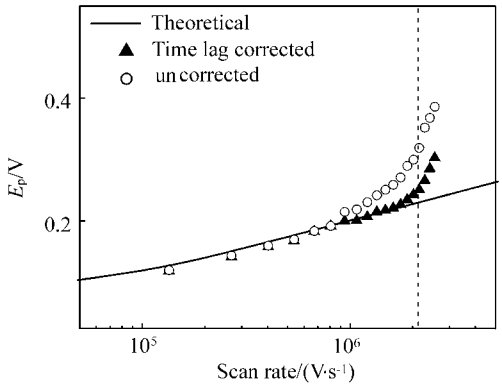


**Figure 8** $\Delta E_p$ as a function of scan rate.

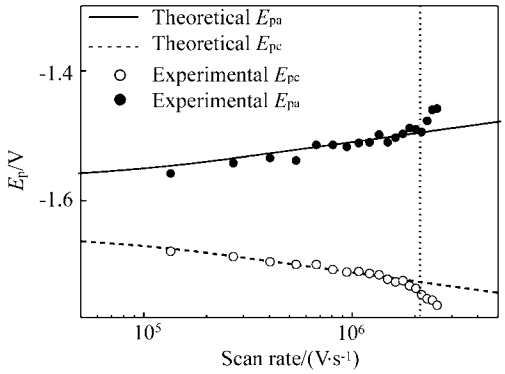


**Figure 9** $E_{pa}$ and $E_{pc}$ as a function of scan rate.

## Acknowledgements

The authors wish to express their great thanks to Dr. Christian Amatore for helpful discussions on the difference between the theoretical solution resistance and the one experimentally determined.

## References

1 Bard, A. J.; Faulkner, L. R. *Electrochemical Methods*: *Fundamentals and Applications*, Wiley, New York, **1980**.
2 Amatore, C.; Maisonhaute, E.; Simonneau, G. *J. Electroanal. Chem.* **2000**, *486*, 141.
3 Amatore, C.; Maisonhaute, E.; Simonneau, G. *Electrochem. Commun*. **2000**, *2*, 81.
4 Amatore, C.; Bouret, Y.; Maisonhaute, E.; Abruna, H.; Goldsmith, J. I. *C. R. Chem*. **2003**, *6*, 99.
5 Garreau, D.; Hapiot, P.; Savéant, J. M. *J. Electroanal. Chem.* **1989**, *272*, 1.
6 Garreau, D.; Hapiot, P.; Savéant, J. M. *J. Electroanal. Chem.* **1990**, *281*, 73.
7 Pospisil, L.; Fiedler, J.; Fanelli, N. *Rev. Sci. Instrum*. **2000**, *71*, 1804.
8 Andrieux, C. P.; Garreau, D.; Hapiot, P.; Pinson, J.; Savéant, J. M. *J. Electroanal. Chem.* **1988**, *243*, 321.
9 Deng, Z. X.; Lin, X. Q. *J. Electroanal. Chem.* **1999**, *464*, 215.

10 Howell, J. O.; Kuhr, W. G.; Ensman, R. E.; Wightman, R. M. *J. Electroanal. Chem.* **1986**, *209*, 77.
11 Baranski, A. S.; Lu, W. *J. Electroanal. Chem.* **1989**, *260*, 1.
12 Amatore, C.; Lefrou, C. *J. Electroanal. Chem.* **1992**, *324*, 33.
13 Wipf, D. O. *Anal. Chem.* **1996**, *68*, 1871.
14 Garreau, D.; Savéant, J. M. *J. Electroanal. Chem.* **1972**, *35*, 309.
15 Wightman, R. M. *Science* **1988**, *240*, 415.
16 Wightman, R. M.; Wipf, D. O. *Acc. Chem. Res.* **1990**, *23*, 64.
17 Andrieux, C. P.; Hapiot, P.; Savéant, J. M. *Chem. Rev.* **1990**, *90*, 723.
18 Zhang, Z. X. *Electrochemistry on Ultramicroelectrodes*, Science Press, Beijing, **1998** (in Chinese).
19 Deng, Z. X.; Lin, X. Q.; Tong, Z. H. *Chin. J. Chem.* **2003**, *21*, 1137.
20 Deng, Z. X. *Ph.D. Dissertation*, University of Science and Technology of China, Hefei, **2000** (in Chinese).
21 Nicholson, R. S. *Anal. Chem.* **1965**, *37*, 1351.
22 Amatore, C.; Lefrou, C. *J. Electroanal. Chem.* **1990**, *296*, 335.

(E0310234 LU, Y. J.)